Electronic Supplementary Material (ESI) for Soft Matter.

Supporting Information: "2D capsid formation within an oscillatory energy landscape: orderly self-assembly depends on the interplay between a dynamic potential and intrinsic relaxation times."

Jessica K. Niblo,[†] Jacob R. Swartley,[†] Zhongmin Zhang,[‡] and Kateri H. DuBay*[,†]

†*Department of Chemistry, University of Virginia, Charlottesville, VA*

‡*Department of Chemistry, University of North Carolina at Chapel Hill, Chapel Hill, NC*

E-mail: dubay@virginia.edu

S1 Additional Methods Details

S1.1 Particle and Inter-particle Interactions Details

The triangular particles are composed of fifteen, partially overlapping circular subparticles that are rigidly held together. Each triangular edge is composed of six subparticles, the outermost of which serve as the vertices of the triangular particle and are shared with the neighboring edge. The triangular particles have an edge length of 1σ, while the subparticles have a diameter of $\sigma_{\mathrm{LJ}} = 0.25\sigma$, where σ is the lengthscale of the system in reduced units.

The subparticles on two edges of the equilateral triangle are assigned type A, while the subparticles on the third edge (including their vertices) are assigned type B. The type

A - type A subparticles of differing triangular particles interact via a Lennard-Jones (LJ) potential, which is illustrated in Figure 1a, and defined as:

$$V_{\mathrm{LJ}}(r_{ij}) = 4\epsilon_{ij}[(\frac{\sigma_{\mathrm{LJ}}}{r_{ij}})^{12} - (\frac{\sigma_{\mathrm{LJ}}}{r_{ij}})^{6}] + c \qquad r_{ij} < r_{\mathrm{c}}, \tag{S1}$$

where r_{ij} is the distance between the centers of an ij-pair, σ_{LJ} is the distance in which the potential goes to zero, and ϵ is the depth of the potential well. For static simulations, ϵ is held constant throughout the simulation, while ϵ is oscillated in time during oscillatory simulations as detailed in the main text. c is the value necessary to shift the potential so that $V_{\mathrm{LJ}}(r_{\mathrm{c}}) = 0$. For type A subparticles, σ_{LJ} defines the spatial extent of the LJ interaction, and the cutoff distance is set so that $r_{\mathrm{c}} = 2.5\sigma_{\mathrm{LJ}}$.

The type B - type B and type A - type B subparticles interact via the Weeks-Chandler-Andersen potential,[S1] which truncates and shifts the LJ potential given in Equation S1 to only include the repulsive portion of the curve where $\frac{\partial U_{ij}(r)}{\partial r} < 0$. In order to truncate and shift the potential, we set $\epsilon_{AB} = \epsilon_{BB} = 1.0$ and $r_{\mathrm{c}} = 2^{1/6}\sigma_{\mathrm{LJ}}$.

S1.2 Simulation Details

All simulations are performed using Langevin dynamics, as implemented in LAMMPS.[S2] Simulations started with a randomly distributed system of 150 triangular particles in a periodic box of size L x L with no particle overlap. Simulations with a volume fraction of $\phi = 0.1$ were done in a box with dimensions 25.48σ x 25.48σ, while simulations at a volume fraction of $\phi = 0.005$ occurred in a box with dimensions of 113.98σ x 113.98σ.

To relax the system, initial velocities were assigned and the simulation was allowed to equilibrate for 1,000,000 steps ($5{,}000\tau$). During this process, all subparticles interacted via the WCA potential, as this ensures there is no particle overlap and establishes an equilibrated random distribution of triangles. After equilibration, the type A attractive interactions were turned on, and the simulation was allowed to proceed for 30,000,000 steps (150,000 τ).

Simulations were evolved in time using the velocity-Verlet algorithm with a timestep of 0.005τ. To mimic solvent dynamics and maintain a constant temperature, the Langevin thermostat was used. The Langevin equation is defined as

$$m\frac{dv}{dt} = -\gamma v - \frac{dU}{dr} + \eta(t). \tag{S2}$$

In addition to the conservative force, $\frac{-dU}{dr}$, that arises from the inter-particle interactions, each triangular particle experiences a friction force and a random force. The friction force is defined as $-\gamma v$, where γ tunes the strength of the friction and v is the velocity describes the frictional interaction between the implicit solvent and the particles. In LAMMPS, we set γ by the *damp* parameter, with $damp = \frac{m}{\gamma}$, where m is mass of the triangular body.[S2] We set $damp = 0.35$ in reduced units. The random force, $\eta(t)$ in Equation S2, mimics the random bumps and kicks the solvent atoms will provide to the subparticle at temperature T. The LAMMPS code was modified so that it used a Gaussian random number for $\eta(t)$ to ensure the appropriate fluctuation statistics.

S1.3 Data Analysis Details

Once the attractive LJ interactions have been turned on, atom positions are recorded every 10τ to monitor the progression of the self-assembly process. To have an even sampling while calculating the final yields, the final $7{,}500\tau$ of each simulation is sampled every 15τ in the static system.

In the temporally variant system, however, sampling the system with a constant interval will result in uneven sampling of the system as it switches between ϵ_{min} and ϵ_{max}. To ensure even sampling between the ϵ_{min} and ϵ_{max} half-cycles during the calculation, the last $7{,}500\tau$ of the simulations is divided into slices of 150τ and ten evenly spaced snapshots from the first complete period of each slice were recorded. For periods equal to or shorter than 0.05τ (ten steps), every step of the first complete period of each slice was recorded to evenly monitor

time within the $\epsilon_{\min}$ and $\epsilon_{\max}$ half-cycles.

S1.3.1 Capsid Counting

To determine the number of assembled capsids, the locations of the type A subparticles that are positioned at the attractive vertex of each triangular particle are compared to the attractive vertices of the other nearby triangular particles. We consider two triangular particles to be part of a potential capsid if the distance between the centers of their attractive vertices are less than 0.85σ. A distance less than 0.85σ was determined to encompass the fluctuations possible in the capsid shape. If any subparticle tip is found to have five neighboring subparticle tips within a distance of 0.85σ, the capsid is considered assembled.

S1.3.2 Aggregate Counting

We also analyze the number of other aggregate structures to better understand the overall assembly process. After determining the number of capsids within the system, the particles that are not within assembled capsids are analyzed to determine what size aggregate they are assembled into. We compare the three vertices of each triangular particle with the three vertices of the nearby particles to determine if the maximum length between any two vertices is less than 2.1σ. A maximum distance of 2.1σ ensures that two particles are assembled, but accounts for all configurations the particles can take in the snake-like aggregates. Aggregates are then built by noting which particles belong to each aggregate.

S2 Temperature in the intermediate period regime

Langevin Dynamics is utilized to move the simulation forward in time and maintain a constant temperature. In LAMMPS,[S2] a Langevin parameter, $damp = \frac{m}{\gamma}$ is defined in units of τ and determines how rapidly the temperature is relaxed to the target temperature.[S2] For oscillation periods similar to the timescale of the damp parameter (0.35τ), the average

temperature of the simulation is higher than the target temperature of 1.0. Figure S1 shows the average temperatures observed in the simulations over the last 5,000τ for a range of oscillation periods as compared to the average temperature for the static potential system. Temperatures at the fast oscillation limit and at oscillations periods longer than 10τ are comparable to those in the static system, but periods from 0.04τ to 5τ deviate more than 5% from the target temperature. To standardize our results for an average ϵ value over the full range of oscillation periods, we report ϵ_{avg} in units of $k_{\text{B}}T^{(\text{obs})}$, where $T^{(\text{obs})}$ is the average observed temperature during the run. This rescaling was only done for Figure 5a&b as no other figures include results from oscillation periods between 0.04τ to 5τ.

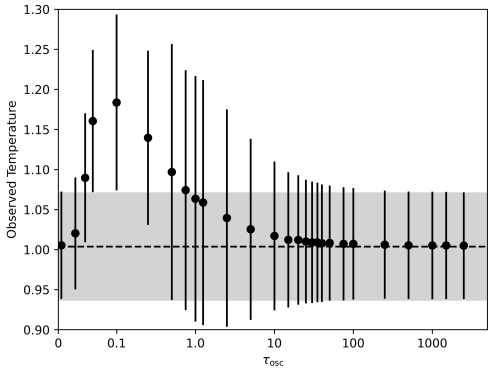

Figure S1: Average observed temperatures at $\epsilon = 1.25k_{\text{B}}T$. The average observed temperature and its standard deviation over the last 5,000τ of the simulation is plotted vs. the oscillation period τ_{osc}. The average observed static temperature is represented by a black dashed horizontal line, and the grey shaded region indicates its standard deviation. We present the average observed temperatures at $\epsilon = 1.25k_{\text{B}}T$ for an amplitude of $0.4k_{\text{B}}T$ as this value is closest to the median ϵ value observed in Figure 5b.

S3 Kinetic traces of structure formation within the static system from $\epsilon = 0.75k_{\text{B}}T$ to $\epsilon = 2.15k_{\text{B}}T$.

In Figure S2 we expand Figure 2b to include additional interaction strengths.

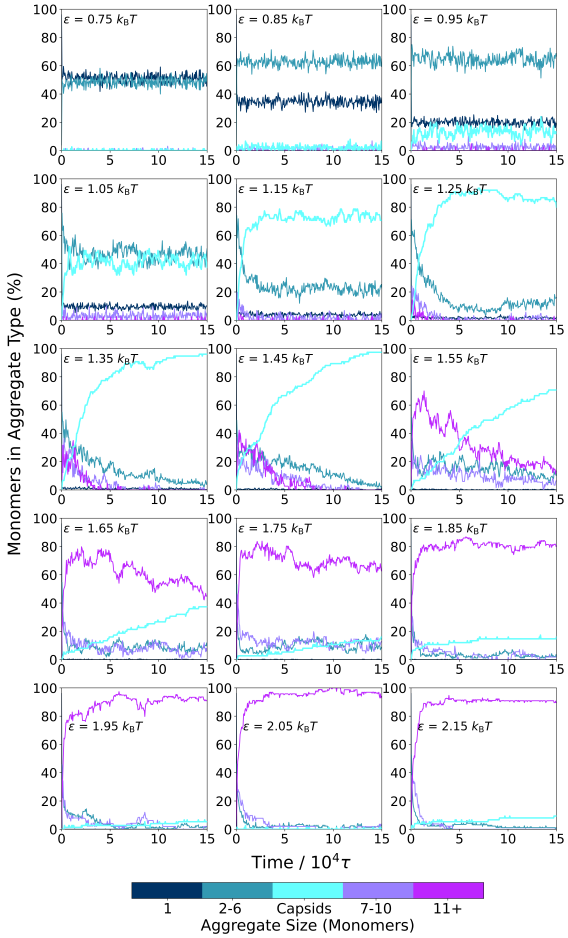

Figure S2: Formation of capsids and aggregates vs. time for different ϵ values in the non-oscillatory system. The formation of various aggregate and capsid species is plotted here vs. time for different ϵ values over a simulation time of 150,000τ. The different aggregate sizes are indicated by the color bar, and the kinetic traces are the average of three independent trajectories.

S4 Mean square displacement and rotational relaxation of a single triangular particle.

We examine the interplay between the oscillation period and the time it takes to diffuse characteristic length-scales that characterize important energetic and structural changes. To quantify particle diffusion, we calculate the mean square displacement for a lone triangle and plot it vs. simulation time in Figure S3a. Additionally, we calculate the rotational

autocorrelation function and plot it against simulation time in Figure S3b. The timescales needed to traverse characteristic distances and rotation are presented in Table 1.

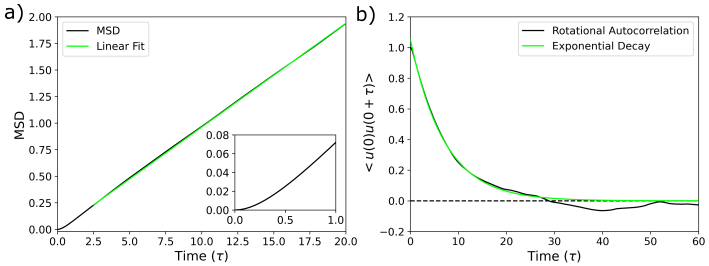

Figure S3: Mean square displacement and orientational autocorrelation function for a single particle. a)The mean square displacement is plotted vs. simulation time for a single triangular particle. Based on the linear fit line in green and the Einstein relation, the diffusion coefficient was calculated to be $D = 0.024 \pm 0.007\sigma^2/\tau$. b) The rotational autocorrelation function for a single triangular particle fit with $N(t) = N_0 exp(-t/\tau)$, where $\tau = 7.103\tau$, and describes the time to decay to $1/e * N_0$. The mean square displacement and rotational autocorrelation function were both calculated from 18 individual trajectories with a recording interval of 0.05τ.

S5 Time averaging in the fast oscillation limit.

Based on earlier work theoretical work by Szleifer and coworkers,[S3,S4] the effective potential in our system can be described at the fast oscillation limit by a static LJ potential with a well depth of ϵ_{avg}, which is simply the time-dependent ϵ value averaged over a single oscillation period.

To show this correspondence, we first write the effective potential at the fast oscillation limit as:

$$U^{\text{eff}}(r) = \int_0^{\tau_{\text{osc}}} U(r, \epsilon(t))dt, \tag{S3}$$

where $U(r, \epsilon(t))$ is the time dependent potential energy of the system at time t, which is integrated over a single oscillation period, τ_{osc}.[S3] We can then substitute in the full LJ potential with a time dependent ϵ on the right hand side, such that:

$$U^{\text{eff}}(r) = \int_0^{\tau_{\text{osc}}} 4\epsilon(t)[(\frac{\sigma}{r})^{12} - (\frac{\sigma}{r})^6]dt. \tag{S4}$$

At the fast oscillation limit, any changes to r during a single oscillation period are small. As a result, Equation S4 becomes

$$\begin{aligned} U^{\text{eff}}(r) &= 4[(\frac{\sigma}{r})^{12} - (\frac{\sigma}{r})^6] \int_0^{\tau_{\text{osc}}} \epsilon(t)dt \\ &= 4 < \epsilon >_{\tau_{\text{osc}}} [(\frac{\sigma}{r})^{12} - (\frac{\sigma}{r})^6], \end{aligned} \tag{S5}$$

where $< \epsilon >_{\tau_{\text{osc}}}$ is the time averaged attraction strength over a single period, which we term ϵ_{avg}.

Finally, since in our simulations, half the oscillation period is spent at ϵ_{max} and half at ϵ_{min},

$$\langle \epsilon \rangle_{\tau_{\text{osc}}} = \frac{\epsilon_{\text{max}} + \epsilon_{\text{min}}}{2} = \epsilon_{\text{avg}}. \tag{S6}$$

S6 Kinetic traces of structure formation with both static and oscillatory interactions.

To investigate in more detail how assembly mechanisms change with oscillatory interactions, in Figure S4 we compare the kinetic traces of the aggregate species in the static system (Column 1) to kinetic traces in the oscillatory system at three different periods. An oscillation period of 0.02τ, which is within the fast oscillation limit, results in very similar assembly to the non-oscillatory system. Intermediate periods, shown in Columns 3 and 4, however, result in very different aggregate assembly kinetics.

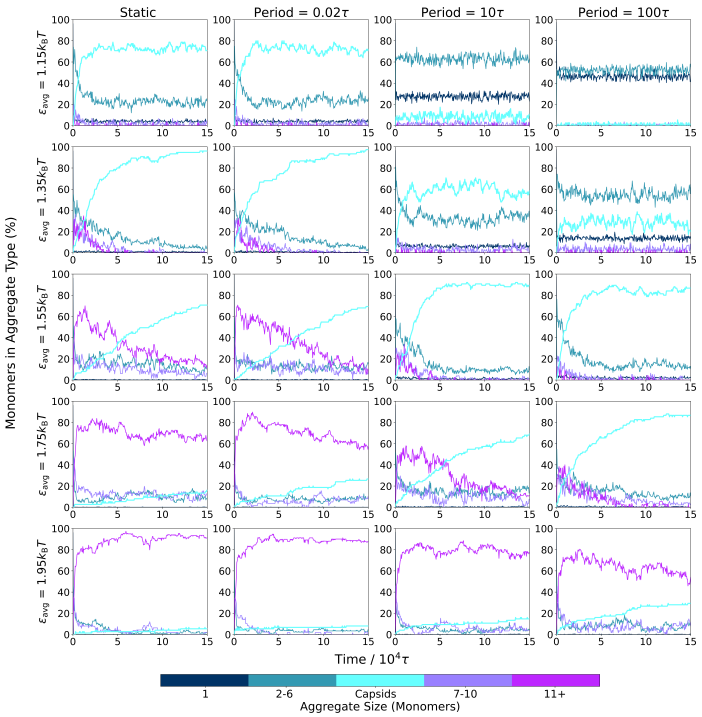

Figure S4: Formation of aggregate species over time for different oscillation periods. The formation of various aggregate species averaged over three indepedent trajectories is shown over time for different ϵ values and oscillation periods at an amplitude of $0.4k_{\mathrm{B}}T$. Column 1 shows results from the static potential system, Column 2 shows results from the fast oscillation limit, and Columns 3 and 4 show results from two different intermediate periods. Different assembled structures are tracked over the simulation as indicated by the color bar.

References

(S1) Weeks, J. D.; Chandler, D.; Andersen, H. C. Role of Repulsive Forces in Determining the Equilibrium Structure of Simple Liquids. *The Journal of Chemical Physics* **1971**, *54*, 5237–5247, DOI: 10.1063/1.1674820.

(S2) Plimpton, S. Fast Parallel Algorithms for Short–Range Molecular Dynamics. *Journal of Computational Physics* **1995**, *117*, 42, DOI: 10.1006/jcph.1995.1039.

(S3) Tagliazucchi, M.; Weiss, E. A.; Szleifer, I. Dissipative Self-Assembly of Particles Interacting through Time-Oscillatory Potentials. *Proceedings of the National Academy of Sciences* **2014**, *111*, 9751–9756, DOI: 10.1073/pnas.1406122111.

(S4) Tagliazucchi, M.; Szleifer, I. Dynamics of Dissipative Self-Assembly of Particles Interacting through Oscillatory Forces. *Faraday Discussions* **2016**, *186*, 399–418, DOI: 10.1039/C5FD00115C.